THE ASTROPHYSICAL JOURNAL, 429:177–191, 1994 July 1

SUPERGIANT MOLECULAR CLOUDS AND THE FORMATION OF GLOBULAR CLUSTER SYSTEMS

WILLIAM E. HARRIS AND RALPH E. PUDRITZ
Department of Physics and Astronomy, McMaster University, Hamilton, Ontario, Canada, L8S 4M1
Received 1992 December 28; accepted 1993 December 23

ABSTRACT

Data from several large elliptical and disk galaxies now show that globular clusters more massive than $\sim 10^5\ M_\odot$ follow a power-law number distribution by mass, $N \sim M^{-1.7}$, which is virtually independent of environment. Within observational uncertainty, this relation is identical to the shape of the mass distributions of giant molecular clouds (GMCs) in large spiral galaxies, the cloud cores embedded in GMCs, and giant H II regions in large spiral galaxies. We interpret this within a model whereby globular clusters formed out of dense cores within supergiant molecular clouds (SGMCs) that were present in the early protogalactic epoch. We construct a theory of pressure confined, self-gravitating, isothermal, magnetized molecular clouds and cores, based on the virial theorem and the observed mass spectra, and derive the characteristic physical properties of these parent SGMCs. These turn out to be of the right mass and density range to resemble the Searle-Zinn primordial fragments from which larger galaxies may have assembled.

We suggest that the protocluster clouds were supported against gravitational collapse primarily by a combination of magnetic field pressure and Alfvénic turbulence, as is observed to be the case for contemporary molecular clouds. This approach removes the need for arbitrary external heat sources (such as long-lasting AGNs or Population III stars) to keep the clouds stable for long enough times to build up to globular-sized masses and more easily permits the global properties of the emergent clusters to be similar from one galaxy to another. By calculating lifetimes through a standard cloud growth model, we estimate that the principal epoch of globular cluster formation should have begun no earlier than a redshift of $z \simeq 6$.

Subject headings: galaxies: formation — globular clusters: general — ISM: clouds

1. INTRODUCTION

Understanding how the old-halo globular clusters formed has been an astrophysically challenging problem for decades, especially because the characteristics of these oldest stellar systems are remarkably similar across all galaxy types and sizes (see Harris 1991 for a recent review). A major clue to this early process must still reside in the luminosity distribution of the globular clusters, which is the visible trace of the cluster mass spectrum. Conventionally, the GCLF (globular cluster luminosity function) is represented as the relative number of clusters per unit absolute magnitude. In such a graph, the GCLF has a characteristic near-Gaussian appearance, in which the "turnover" or peak frequency (at $M_V \simeq -7.2$) and the sample dispersion ($\sigma \simeq 1.4$ mag) are similar to within ± 0.2 mag in all the galaxies studied to date (Harris 1993). Plotted in this way, the shape of the GCLF is suggestive of a characteristic cluster luminosity which other authors have postulated to represent the Jeans mass in the protogalactic gas (e.g., Peebles & Dicke 1968; Fall & Rees 1985, 1988; Kang et al. 1990; Murray & Lin 1992).

An alternative and more physically based representation of the GCLF is the number of clusters per unit *mass* or luminosity. Richtler (1992) has recently emphasized that the majority of the Milky Way globular cluster population fits a simple power-law distribution when plotted in this way. Surdin (1979) appears to have been the first to describe the mass spectra of globular clusters as power laws, suggesting that $N(M)$ (the number of clusters per unit mass) behaves as $N_\oplus \propto M^{-1.9}$ in the Milky Way for masses $5 < \log (M/M_\odot) < 6.3$ and the much shallower distribution $\propto M^{-0.75}$ for low-mass clusters, $4.2 < \log (M/M_\odot) < 5$. Racine (1980) also proposed $N_\oplus \sim M^{-2}$ at least for the brighter clusters in the Milky Way and M31. Both of these early discussions employed much less complete and accurate databases than exist today. Richtler (1992), using Webbink's (1985) catalog for the Milky Way globular clusters, recovered Surdin's value of -1.9 for the mass spectral index. A power-law spectrum has no characteristic mass scale. Thus, the relevance of the Jeans-mass argument is less evident if this same observational result is found to hold for globular clusters in galaxies generally.

The GCLF observed today must be a result of both the orignal mass spectrum of cluster formation and the subsequent dynamical evolution of the clusters due to processes such as dynamical friction, early mass loss, tidal shocking by the galactic bulge or disk, and stellar evaporation coupled to the surrounding tidal field (e.g., Surdin 1979; Aguilar, Hut, & Ostriker 1988; Ostriker 1988; Chernoff & Weinberg 1990). However, both tidal shocking and dynamical fraction are relatively ineffective outside of ~ 2 kpc of the Galactic center, so that all but the smallest of the halo clusters beyond this central bulge region should have been little affected. In addition, stellar evaporation may actually be reduced by the galactic tidal field through its circularizing effect on the orbits of stars in the outer parts of the clusters (Oh & Lin 1992); and the recent discovery that typical halo clusters may have much larger amounts of mass in lower main-sequence stars than was previously realized (Richer et al. 1991; Leonard, Richer, & Fahlman 1992) considerably reduces the expected disruptive effects from stellar evolution of high-mass stars in the first $\sim 10^8$ yr of the clusters' history. In summary, reasonable evidence now exists—at least for the majority of the halo cluster population—that the present-day mass distribution of the globular clusters fairly reflects the shape of their formation spectrum (see Murray & Lin 1992, 1993).

In addition, stellar systems as massive as the old globular clusters did not form only in the pregalactic or protogalactic epoch. Although rare, star clusters younger than ~ 1 Gyr and with masses comparable to classic globulars are to be found in environments as diverse as the LMC (e.g., Fischer et al. 1992; Mateo 1993; Larson 1993), the blue compact dwarf NGC 1705 (Meurer et al. 1992), the recent merger product NGC 3597 (Lutz 1991), and the supergiant NGC 1275 with its highly active nuclear region (Holtzman et al. 1992), among other locations. These data support the view that the physical characteristics of star clusters everywhere (age, mass, metallicity) form a general continuum even though the highest mass ones may have formed most frequently at the earliest epochs (see Larson 1990, 1992, 1993 for further comments).

In this paper, we investigate the connection between protogalactic and present-day cluster formation by examining the GCLF data for several large galaxies in addition to the Milky Way. We then compare them with the strikingly similar power-law mass spectra that describe the sites of *present-day* cluster formation: GMC's, cloud cores, and giant H II regions. By constructing a theoretical model based on the virial theorem and applied to pressure confined, magnetized self-gravitating clouds, we then predict the mean properties of the primitive parent clouds (which we call supergiant molecular clouds or SGMCs) in which the protoglobular cores were likely to have formed.

2. THE OBSERVED CLUSTER MASS SPECTRUM

We first investigate the *observed* number distribution of globular clusters by mass in several large galaxies for which the available data permit accurate definitions of the GCLF. For the Milky Way, we use the recent list of cluster distances and integrated magnitudes described by Harris et al. (1991) and Secker (1992), with a few more updates for individual clusters. From this catalog we extract 102 globular clusters with known Galactocentric distances from 2 to 40 kpc, and convert their measured integrated luminosities M_V into masses using a mean mass-to-light ratio $(M/L)_V = 2.0$ (Mandushev, Spassova, & Staneva 1991). Although the few globular clusters with galactocentric distances less than 2 kpc do not follow a noticeably different GCLF (cf. Armandroff 1989), we exclude them for the dynamical reasons mentioned above. We also exclude the handful of low-luminosity Palomar-type clusters in the outermost halo ($R_{gc} > 40$ kpc), although (as will be evident later) adding them in would not affect any of our conclusions. Our adopted sample of Milky Way halo clusters is, then, a *complete* spatially defined sample that is least likely to have been eroded significantly by dynamical processes.

Figure 1 shows the resulting histogram of this sample, binned in steps of $5 \times 10^4\ M_\odot$. For $M \gtrsim 10^5\ M_\odot$, the mass distribution mimics a power-law falloff $N_\oplus \propto M^{-\alpha}$ rather accurately. At masses less than $M_{min} \sim 10^5\ M_\odot$, the relative numbers of clusters remain roughly constant per (equal-mass) bin. (A graph of log N against log M should exhibit a straight line falloff of slope α; however, the small sample size here and the large total mass range leave many of the higher mass bins empty, so that the linear (N vs. M) form of the graph is more useful in this case.) We determine the exponent α by a simple one-parameter maximum likelihood solution, which is independent of any particular binning. Table 1 shows our numerical results for three different choices of M_{min}. (Throughout the table, the quoted uncertainties are the $\pm 90\%$ error margins.) Lower cutoff values M_{min} necessarily lead to shallower slopes α: the "best" choice of M_{min} is debatable, but cannot be much lower than $\sim 0.75 \times 10^5\ M_\odot$, below which the mass histogram clearly levels off.

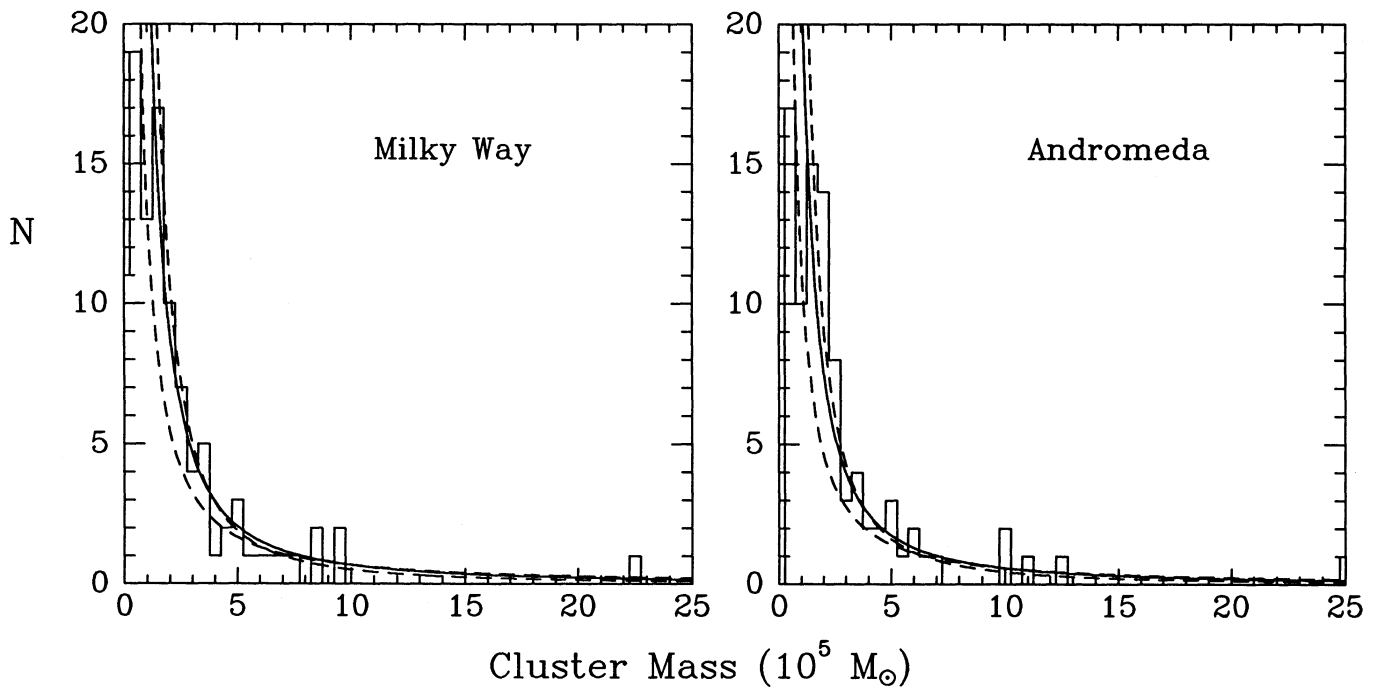

FIG. 1.—(*left*) Mass distribution for the globular clusters in the Milky Way halo, with data as listed by Secker (1992). Here N is the number of clusters per $0.5 \times 10^5\ M_\odot$ bin. The *solid line* is the power-law mass distribution $N \sim M^{-\alpha}$ with $\alpha = 1.6$ (see § 2 of the text). The dashed lines show similar fits for $\alpha = 1.3, 1.9$. (*Right*) The mass distribution for a complete sample of globular clusters in the M31 halo. The fitted curves are the same as for the Milky Way.

TABLE 1

MASS SPECTRAL INDICES FOR GLOBULAR CLUSTER SYSTEMS

Galaxy	M_{min} ($10^5 M_\odot$)	α	Reference
Milky Way	0.50	1.52 ± 0.13	1
	0.75	1.69 ± 0.17	
	1.00	1.96 ± 0.20	
M31	0.50	1.52 ± 0.13	1
	0.75	1.70 ± 0.16	
	1.00	1.88 ± 0.19	
M87 (*V*)	1.40	1.60 ± 0.02	2
3 Virgo E's (*B*)	1.00	1.61 ± 0.03	3
NGC 1399 (*V*)	0.80	1.61 ± 0.20	4
NGC 1399 (*B*)	1.00	1.58 ± 0.20	
NGC 4594 (*B*)	0.62	1.54 ± 0.10	5

REFERENCES.—(1) Secker 1992; (2) McLaughlin et al. 1994; (3) Harris et al. 1991; (4) Bridges et al. 1991; (5) Bridges & Hanes 1992.

An especially useful comparison of the Milky Way data can be made with M31 (Andromeda), in which a halo-cluster sample that is very nearly complete and uncontaminated has recently been constructed (Racine 1991; Reed, Harris, & Harris 1991; Racine & Harris 1992; see Secker 1992 for a summary list). This M31 sample excludes the inner-spheroid and outermost-halo clusters in very much the same way as in the Milky Way discussed above and is plotted in Figure 1*b* with the same assumptions as before [$(M/L)_V = 2$, bin size $0.5 \times 10^4\ M_\odot$]. The maximum-likelihood results for α are listed in Table 1. For a given M_{min}, the similarities between the Milky Way and M31 globular cluster mass distributions are striking.

The GCLFs for selected giant elliptical galaxies can also be added to our comparative study. Recent data from Harris et al. (1991) provide such material for three Virgo gE's (NGC 4365, 4472, and 4649) to a limiting magnitude $M_V \simeq -6$, corresponding to mass $M \simeq 0.5 \times 10^5\ M_\odot$. The GCLFs for these are published as the residual numbers of globular clusters per unit magnitude after correction for photometric incompleteness and subtraction of the contaminating background LF. For our purposes, we reconvert each bin total to the relative number of clusters per unit *mass*, and combine all three into a single LF since the analyses of Harris et al. (1991) and Secker & Harris (1993) demonstrate that their GCLFs are similar to one another within the observational uncertainties (the NGC 4365 LF was first adjusted for a distance modulus difference of 0.8 mag relative to the other two Virgo members; see Tonry, Ajhar, & Luppino 1990 and Secker & Harris 1993). Figure 2 shows that a power law adequately describes the main population of clusters, although these data do not reach faint enough to show more than a clear hint of the flattening at the low-mass end. At the very top end, which extends to higher mass than the Milky Way or M31 clusters because of its much larger sample size, there is a steeper downturn beginning at $M_{max} \simeq 3 \times 10^6\ M_\odot$. A weighted least-squares fit to the data points (in this case, for the mass range $M_{min} < M < M_{max}$) gives the value for the logarithmic slope α listed in Table 1.

The GCLFs from two cD ellipticals, M87 in Virgo (McLaughlin, Harris, & Hanes 1994) and NGC 1399 in Fornax (Bridges, Hanes, & Harris 1991), are also shown in Figure 2. These are of special interest because of their high specific frequencies, with cluster populations almost 3 times higher than normal for the luminosity of the host galaxy. Although the photometric limits for these two galaxies ($M_V \simeq -7.5$, or $M_\oplus \simeq 1.7 \times 10^5\ M_\odot$) do not reach quite as deep as for the normal Virgo E's listed above, accurate solutions for α are obtainable because of the very large sample sizes. In particular, the M87 data (McLaughlin et al.) are based on a sample of almost 3000 clusters and thus extend to very high luminosity, clearly revealing the top-end breakpoint M_{max} above which the slope unambiguously steepens. For $M > M_{max}$, direct least-squares fits to the M87 and Virgo gE data points yield a slope $\alpha_2 = 3.2 \pm 0.5$ (estimated error).

Last, we add to Figure 2 the GCLF for the giant Sa galaxy NGC 4594 (Bridges & Hanes 1992).

As is seen in Table 1, the mass spectral indices for *all* the GCLFs studied—large disk galaxies, giant ellipticals, and cD's—are remarkably similar. The small but very clean and well defined cluster samples from the Milky Way and M31 will form our baseline reference for the ensuing discussion. From them, we adopt $\alpha \simeq 1.7 \pm 0.1$ as providing a near-universal match to the mass spectrum of the globular clusters over the range $M_{min} \simeq 10^5\ M_\odot$ up to $M_{max} \simeq 3 \times 10^6\ M_\odot$.

3. OBSERVED PROPERTIES OF GMCS AND THEIR CORES

3.1. *Mass Spectra and Physical Properties*

Several lines of observational evidence show that a similar spectral index α describes both the mass spectra of giant molecular clouds (GMCs) and their internal dense cores that are sites of *current* star cluster formation. It is remarkable that this correlation spans nearly *6 decades* in mass (from 1 to $10^6\ M_\odot$)

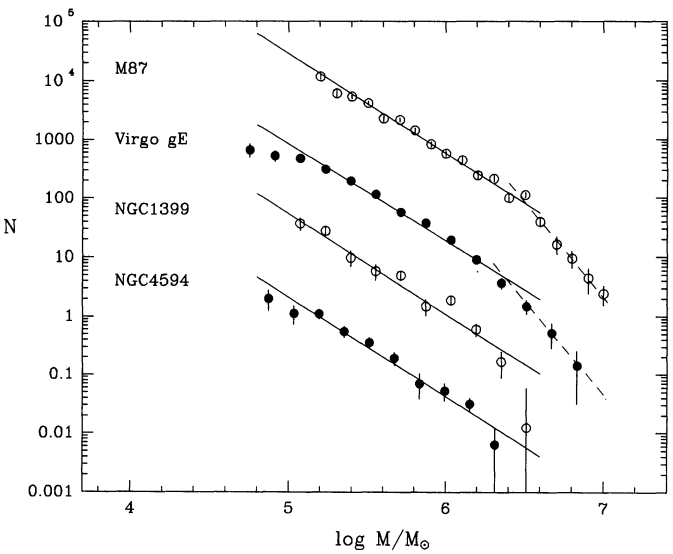

FIG. 2.—Mass distributions for the globular clusters in selected large galaxies as described in § 2 of the text. The number of clusters in each mass bin is plotted against mass M in log-log form; the four data sets are plotted with arbitrary vertical offsets for clarity. From the top down, the four curves represent (1) a large sample of the bright clusters in M87, from McLaughlin et al. (1984); (2) data for three other Virgo Cluster ellipticals combined, from Harris et al. (1991); (3) the GCLF for the Fornax cD galaxy NGC 1399, from Bridges et al. (1991); and (4) the GCLF for the Sombrero giant Sa galaxy (NGC 4594), from Bridges & Hanes (1992). The solid lines drawn through each set of points all have slopes $\alpha = \Delta \log N/\Delta \log M = 1.7$, and the dashed lines drawn through the high-mass ends of the Virgo elliptical GCLFs have slopes $\alpha_2 = 3.2$.

and that clouds and cores over this enormous span also appear to be structures in virial equilibrium.

1. Complete CO surveys of the Milky Way reveal that approximately half of the ISM gas is contained in discrete GMCs with masses in the range $2 \times 10^6 \geq M_{\rm GMC} \geq 10^5\ M_\odot$ (Sanders, Scoville, & Solomon 1985, hereafter SSS; Scoville & Sanders, 1987). The spectrum of measured cloud diameters D is characterized by a power-law $N_{\rm GMC}(D) \propto D^{-2.32\pm0.25}$, and the one-dimensional internal velocity dispersion of the clouds varies as $\sigma_v(D) \propto D^{0.55\pm0.05}$. The GMCs appear to be in virial equilibrium (e.g., Fleck 1988; Elmegreen 1989; McKee 1989; SSS), so that the cloud masses may be deduced from $M \propto D\sigma_v^2$. The mass spectrum which results is $N_{\rm GMC}(M) \propto M^{-\alpha}$ with $\alpha = 1.63 \pm 0.12$, and the mean cloud density varies with diameter as $n \propto D^{-0.9}$. The *median* cloud (see § 4 below for definition) in this GMC spectrum has the properties summarized in Table 2 [we have used a coefficient of 5 in the virial theorem linking cloud radius r, one-dimensional velocity dispersion σ, and mass (see eq. [5.1] to follow), while Scoville & Sanders use 6].

Similar results hold for GMCs in other galaxies as well. The most complete such study is that of M33 by Wilson & Scoville (1990), who find sizes and velocity dispersions nearly identical with the Milky Way, and an associated cloud mass spectrum with $\alpha = 1.5 \pm 0.2$ (Wilson, private communication). Recent observations of molecular clouds in the LMC and SMC indicate, moreover, that the size-linewidth relations there are identical to that of the Milky Way, although the CO to H_2 conversion factor may be somewhat higher (Johansson 1991; Rubio, Lequeux, & Boulanger 1993). The fact that these scalings hold for the LMC and SMC is important since their lower metallicity may more closely resemble star formation conditions in protogalaxies and in other present-day systems such as blue compact dwarfs.

2. Modern surveys of molecular clouds reveal that they are highly filamentary structures containing many embedded clumps and cores (Bally et al. 1987; Castets et al. 1990; Duvert, Cernicharo, & Baudry 1986). The clumps within such clouds follow well-defined power-law distributions in their physical properties: for example, Lada, Bally, & Stark (1991) find for the Orion cloud ($M_{\rm cloud} \simeq 10^5\ M_\odot$) that the core mass function has a spectral index $\alpha = 1.6$. The first high-resolution survey of another section of the Orion cloud identifies 125 clumps which have an identical mass function (Tatematsu et al. 1993). Blitz (1991) summarizes the distribution of clump masses embedded within six very different molecular clouds (Orion B, Ophiuchus, Cepheus, and others). The mass spectral index of the clumps is $\alpha_{\rm cl} \simeq 1.6 \pm 0.16$ over three decades in mass (1–3000 $M_\odot$). There is good evidence that these molecular cloud cores are also in virial equilibrium and are characterized by similar scaling laws as for GMCs, namely $\sigma_{v,\rm core} \propto r^{0.5}$ and $M_{\rm cor} \propto r^2$ (Larson 1981).

We deduce the properties of the median GMC core—to be used later in our discussion—from the data compiled by Friberg & Hjalmarson (1991) and Goldsmith (1987). These reviews indicate that the cores of GMCs have masses in the range 10^1–$10^3\ M_\odot$; radii from 0.25 to 1.5 pc; velocity dispersions of 1 to 3 km s^{-1}; and densities in the range 10^4–10^6 cm^{-3}. We take the maximum mass of the GMC cores to be $3 \times 10^3\ M_\odot$ and deduce the median parameters listed in Table 2. These data show that the median core mass is much smaller than that of its parent molecular cloud; specifically, from Table 2,

$$\eta \equiv \bar{M}_{\rm core}/\bar{M}_{\rm cloud} \simeq 10^{-3}\ , \qquad (3.1)$$

We will use this core mass ratio in the modeling discussion to follow.

3. The luminosity functions of giant H II regions in large spiral galaxies such as M51 and M101 (e.g., Kennicutt 1989; Scowen, Dufour, & Hester 1992; Rand 1992) show the same power-law shape as for the GMCs and cores, with α in the range 1.6–1.9. With the reasonable assumption that the total H II region luminosity is proportional to the stellar mass present, we again derive the same mass spectrum slope.

The two central observational facts about GMCs and their cores are that they obey the same size-linewidth relation ($\sigma \propto r^{1/2}$) and have nearly constant column densities ($N \equiv M/\mu m_p \pi r^2 \simeq$ const, where $\mu = 2.3$ is the mean molecular weight of the gas and m_p is the proton mass). As noted previously, these results are consistent with virial equilibrium for the clouds (Elmegreen 1989; Fleck 1988; and § 5 below).

3.2. *Internal Dynamics of Clouds and Their Cores*

The observed CO line widths of GMCs are of the order of their virial velocities, so that they are universally strongly suprathermal. Observations clearly show that both thermal pressure and rotation have energy densities that are at least an order of magnitude smaller than the gravitational energy density of clouds. However, magnetic fields in molecular clouds have energy densities comparable to their gravitational potential energy density (see, e.g., Myers & Goodman 1988, and the excellent review by McKee et al. 1993), and there is mounting observational evidence that molecular clouds are supported by the pressure from both an ordered and a disordered magnetic field.

Molecular clouds have internal pressures far larger than the pressure of the surrounding hot ISM (e.g., Elmegreen 1989). The reason is that molecular clouds are self-gravitating. The ratio of cloud internal pressure $P_c = G\Sigma_c^2$ to external pressure $P_{\rm ISM}$ is ~ 30 for the gamut of GMCs in the Milky Way. This large pressure is maintained by nonthermal motions in the GMC, whose origin is gravitational or hydromagnetic in nature.

Finally, we note that the smallness of the ratio $\eta \sim 10^{-3}$ (eq. [3.1]) can also be understood as a consequence of the virial theorem. Cores are far less turbulent than the surrounding GMC in which they are embedded. Now, the virial theorem predicts that $M \propto \sigma^4$, so that $\eta = (\sigma_{\rm core}/\bar{\sigma}_{\rm cloud})^4$, and using the velocity dispersions in Table 2, we recover the ratio given in equation (3.1). The cores are in pressure balance with the GMC gas in which they are embedded because they are much denser; thus, their pressure $\rho_{\rm core}\sigma_{\rm core}^2$ is comparable with that of the surrounding more turbulent gas.

TABLE 2

OBSERVED MEDIAN CORE AND CLOUD PROPERTIES FOR GALACTIC GMCs

Parameter	Median Core	Median Cloud
$\bar{M}\ (M_\odot)$	5.4×10^2	3.3×10^5
$\bar{r}$ (pc)	0.38	20
$\bar{n}\ (cm^{-3})$	4.1×10^4	170
$\bar{\rho}\ (M_\odot\ pc^{-3})$	2.3×10^3	9.8
$N\ (10^{22}\ cm^{-2})$	6.5	1.4
$\Sigma\ (M_\odot\ pc^{-2})$	1.2×10^3	260
$\bar{\sigma}_v\ (km\ s^{-1})$	1.1	3.8

4. IMPLICATIONS OF GLOBULAR CLUSTER MASS SPECTRA

The wide range of observational material summarized above leads repeatedly to mass spectral indices $\alpha = 1.6$–1.7 for GMCs, cloud cores, giant H II regions, and globular clusters. In total, *the data are highly suggestive of the view that globular clusters formed with the same type of mass distribution, and in the same way, as star clusters are forming today.* We proceed with this assumption to develop a theory for SGMC clouds and their cores using the same physical principles relevant to contemporary clouds. We specifically identify protoglobular clusters as the *gaseous cores* within the hypothetical SGMCs.

4.1. *A Growth Model for Protocluster Clouds*

Spectral indices α in the range $\simeq 1.5$–1.8 can be successfully reproduced by a model in which small clouds coalesce into large ones by simple collisions, as has frequently been demonstrated (e.g., Field & Saslaw 1965; Kwan 1979; Kwan & Valdes 1983; Elmegreen 1987; Carlberg & Pudritz 1990). Kwan (1979) has derived useful analytical and numerical results for the mass spectrum of clouds growing by agglomeration, which for convenience we briefly summarize here. Consider an initial collection of clouds of some small mass M_0. At any mass M, the rate of loss of $N(M)$ is due to collisions with other clouds, while the rate of gain of $N(M)$ is due to binary collisions of clouds of smaller mass. Clouds that grow to masses exceeding some value M_1 suffer disruption due to processes related to star formation; that is, a given fraction of all clouds with mass in excess of M_1 are disrupted in a characteristic time τ. The disruption regenerates a collection of small clouds of mass M_0, and in statistical equilibrium the mass spectrum reaches a steady state. The resulting mass spectrum is *insensitive* to M_0 for masses $M \gtrsim 10M_0$.

The geometric cross section and velocity of a cloud of mass M are expressed as power laws of the cloud mass; i.e., $\sigma_M = \sigma_0(M/M_0)^a$, and $v_M = v_0(M/M_0)^b$. In steady state, equipartition of kinetic energy among the colliding and coalescing clouds is established so that $b = -\frac{1}{2}$. The detailed numerical solutions show that collisions between two massive clouds are infrequent, and that a massive cloud grows by accreting *smaller* clouds. The important cross-section is therefore just the geometric cross section of the larger clouds. If the clouds have uniform density, then we have $a = \frac{2}{3}$ for the geometric cross section. However, the clouds that would build up our SGMCs might be massive enough to be themselves self-gravitating. If so, they would have a constant surface density (cf. eq. [5.3] below), for which the geometric cross section is $a = 1$.

Within the preceding physical picture there are two regimes for which analytic solutions to the mass spectrum in statistical equilibrium are known (see Kwan 1979): for clouds whose growth times are *shorter* than their lifetime τ, the mass spectrum is a power law with the index

$$\alpha = (3 + a + b)/2 . \tag{4.1}$$

Thus with $b = -\frac{1}{2}$, the mass spectral indices range from $\alpha = 1.59$ (for $a = \frac{2}{3}$) to $\alpha = 1.75$ (for $a = 1$). Our observational determination $\alpha = 1.7 \pm 0.1$ falls comfortably within this predicted range.

The number of the most massive clouds whose growth times are *longer* than their lifetime τ takes a sharp down-turn. In this regime, the mass spectrum takes the general form $N(M) = \sigma_M^{-1} \exp\left[-\beta \int (\sigma_0/\sigma_M) d(M/M_0)\right]$, where the coefficient β is defined below. For the particular case where the cross section is $a = 1$, the mass spectrum again becomes a power law:

$$N(M) \propto M^{-(1+\beta)}, \quad \beta \equiv \frac{M_0}{\langle\rho\rangle \sigma_0 v_0 \tau} . \tag{4.2}$$

In equation (4.2), the growth time of clouds—essentially, the mean time between collisions—is $\simeq M_0/\langle\rho\rangle\sigma_0 v_0$ and therefore the index β measures the ratio of the cloud growth time to the cloud lifetime τ. Thus, measuring the slope of the mass function in the highest mass portion of the spectrum allows one to estimate the time scale for cloud formation. We identify β with our observationally determined index α_2 (Fig. 2 and § 2) through the obvious relation $\beta = (\alpha_2 - 1) \simeq 2.2$.

4.2. *Properties of the Observed Mass Spectra*

Now consider a mass spectrum of the specific form

$$\begin{aligned} N(M) &= \text{constant} \ (M < M_{\min}) \\ &= kM^{-\alpha} (M_{\min} < M < M_{\max}) \\ &= kM_{\max}^{\alpha_2 - \alpha} M^{-\alpha_2} (M > M_{\max}) . \end{aligned} \tag{4.3}$$

This form of the mass distribution is chosen to approximate the *present-day* GCLFs as shown in Figures 1 and 2; and a schematic version of this distribution is shown in Figure 3. Then the following relations may quickly be shown (see also Ashman & Zepf 1992 for a similar derivation in a slightly different context):

total number of clouds:

$$N_T = \frac{k}{(\alpha - 1)} \left(\alpha M_{\min}^{1-\alpha} - \frac{\alpha_2 - \alpha}{\alpha_2 - 1} M_{\max}^{1-\alpha} \right) , \tag{4.4}$$

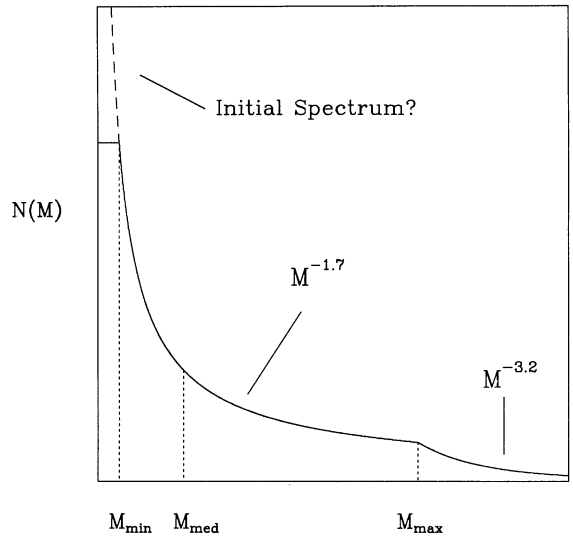

FIG. 3.—Schematic definition of the fiducial mass spectrum of globular clusters or protocluster clouds. The solid line shows the relative number $N(M)$ of clouds at mass M, over three distinct mass ranges: for $M < M_{\min}$, the number of clouds is constant; for $M_{\min} < M < M_{\max}$, it follows the power-law $M^{-\alpha}$ for the equilibrium model of cloud growth by collisions; and for $M > M_{\max}$ it follows the steeper power law $M^{-\alpha_2}$ applicable to very massive clouds whose growth time is shorter than their lifetime against star formation. The observational constraints from Fig. 2 give $\alpha = 1.7$ and $\alpha_2 \simeq 3.2$. The median cloud mass is also marked, as defined in eq. (4.6) of the text. For the low-mass end, we suppose that the initial mass spectrum may have extended upward with the same power law (*dashed line*) but that over a Hubble time most of these small clusters have been disrupted (see text). The spectrum shown here is schematic only and is not plotted accurately to scale; compare with Fig. 1.

total cloud mass:

$$M_T = \frac{k}{(2-\alpha)}\left(-\frac{\alpha}{2}M_{\rm min}^{2-\alpha} + \frac{\alpha_2-\alpha}{\alpha_2-2}M_{\rm max}^{2-\alpha}\right). \quad (4.5)$$

Now also define $\bar{M}$ such that half the total mass of the entire distribution is contained in clouds more massive than $\bar{M}$. Then if $M_{\rm min} \ll M_{\rm max}$ as the actual data indicate, we have

$$\text{median mass: } \bar{M} \simeq \left[\frac{\alpha_2-\alpha}{2(\alpha_2-2)}\right]^{1/(2-\alpha)} M_{\rm max}\,, \quad (4.6)$$

and the number of clouds with M greater than the median mass is

$$N(>\bar{M}) = \frac{(2-\alpha)}{2(\alpha-1)} \times\left\{1-\left(\frac{\alpha_2-\alpha}{\alpha_2-1}\right)\left[\frac{2(\alpha_2-2}{\alpha_2-\alpha}\right]^{(1-\alpha)/(2-\alpha)}\right\}\frac{M_T}{\bar{M}}\,. \quad (4.7)$$

Let us now apply these general relations to the observed globular cluster distribution. If we adopt $\alpha = 1.7$, $\alpha_2 = 3.2$ along with $M_{\rm min} \simeq 10^5\ M_\odot$, $M_{\rm max} \simeq 3 \times 10^6\ M_\odot$, then equations (4.6) and (4.7) become

$$\bar{M}_\oplus \simeq 0.21 M_{\rm max} \simeq 6.3 \times 10^5\ M_\odot\,,$$
$$N(>\bar{M}) \simeq 0.17 M_T/\bar{M}\,. \quad (4.8)$$

The same data show that the central part of the mass distribution ($M_{\rm min} < M < M_{\rm max}$) contains two-thirds of the total mass M_T; the high end $M > M_{\rm max}$ contains slightly more than a quarter of the total; and the low-mass end $M < M_{\rm min}$ contains less than 6% of the total.

From the arguments summarized earlier, we assume that the globular cluster mass distribution, for $M \gtrsim M_{\rm min}$, represents *the direct trace of the cluster formation spectrum.* The shape of the low-mass portion ($M < M_{\rm min}$), where the number of globular clusters per unit mass remains roughly uniform, may also preserve much of the initial mass spectrum except at very low masses ($\lesssim 10^4\ M_\odot$). Obviously, at low enough masses the various destructive mechanisms within the tidal field of the galaxy will begin to play a role. However, it is important to realize that even if there originally existed a much larger population of low-mass clusters that has now mostly dissolved, these putative "lost clusters" *cannot have contributed much to the total field star population* because of their small size. For example, even if we assume that the initial cloud mass spectrum extended down all the way to $M_{\rm min} = 0$ with the same index $\alpha = 1.7$, then equation (4.5) shows that M_T increases by just 30% over its present-day value. Thus it is quite unlikely that much of the Galactic halo was built out of "dissolved" globular clusters (see also Harris 1991 for a summary of other arguments toward the same conclusion).

It is worth noting here how this power-law representation of the cluster mass distribution relates to the traditionally used Gaussian model of the GCLF. Figure 4 illustrates this comparison for a representative example. Here, we display a random sample of ~200 clusters generated with the mass distribution of equation (4.3), using parameters ($M_{\rm min}$, $M_{\rm max}$, α) appropriate for the galaxies described above. The cluster masses were then individually converted to absolute magnitude M_V, and replotted as number per 0.4 magnitude bin. The net distribution satisfactorily fits a Gaussian-like curve in $N(M_V)$ with parameters appropriate for the Milky Way or M31 (Secker 1992). The "turnover" at $M_V \simeq -7$ and the decrease in the cluster numbers at fainter magnitudes (where in fact the number of clusters per unit *mass* is staying roughly constant) arise from the logarithmic rebinning process *combined with the flattening of the original mass distribution for* $M < M_{\rm min}$. As one would intuitively expect, the GCLF turnover point is the image of $M_{\rm min}$. In summary, there is no basic discrepancy between the two formulations; each is useful in a different context. A more detailed discussion of the analytic relations between these two forms of the GCLF is given by McLaughlin (1994).

4.3. *Minimum Mass of Cores in Galactic SGMCs*

In order to produce bound stellar clusters within clouds that can generate OB stars, the efficiency of star formation *in the core gas* must be $\epsilon \gtrsim 0.5$ (e.g., Lada, Margulis, & Dearborn 1984). Since the star formation is unlikely to be 100% efficient, we henceforth denote for convenience the star formation efficiency as $\epsilon = 0.75\epsilon_f$ with $\epsilon_f \sim 1$. Thus the progenitor SGMC must have had cloud cores with median masses $\bar{M}_{\rm core} \simeq \epsilon^{-1}\bar{M}_\oplus = 8.4 \times 10^5 \epsilon_f^{-1}\ M_\odot$. The median cores in SGMCs were then a factor of at least

$$\bar{m}_{\rm core} \equiv (\bar{M}_{\rm core,SGMC}/\bar{M}_{\rm core,GMC}) = 1.6 \times 10^3 \epsilon_f^{-1} \quad (4.9a)$$

more massive than their contemporary counterparts in the Milky Way disk. This ratio must be a *lower limit* because it does not account for mass loss from within the clusters (gas loss, stellar evaporation, tidal truncation) over the age of the Galaxy, which even for massive clusters may be typically a factor of ~2 (e.g., Chernoff & Weinberg 1990; Lee, Fahlman, & Richer 1991; Johnstone 1993). However, the high efficiency of star formation in the most massive cloud cores guarantees

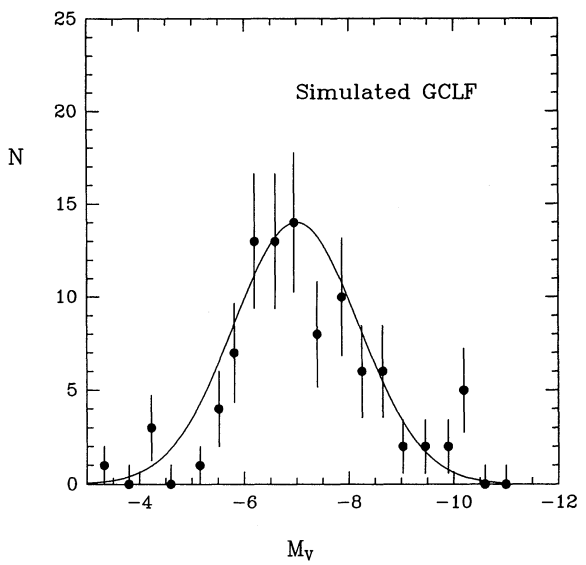

FIG. 4.—A simulated globular cluster luminosity distribution (GCLF), generated from the power-law formulation of eq. (4.3) but plotted in the traditional observational form as number of clusters per unit magnitude. Here, ~200 clusters were selected randomly from the power-law distribution, with $M_{\rm min} \simeq 8 \times 10^4\ M_\odot$, $M_{\rm max} \simeq 3 \times 10^6\ M_\odot$, and $\alpha = 1.7$ as described in the text. Masses were converted back to absolute magnitude with $(M/L)_V = 2$. The plotted points give the number of clusters per 0.4 mag bin, with error bars equal to $N^{1/2}$. A Gaussian curve with peak at $M_V = -7$ and standard deviation $\sigma = 1.2$ mag (appropriate for the Milky Way GCLF) is superposed on the points for comparison.

that the emergent cluster mass spectrum is effectively the progenitor cloud core spectrum.

The median mass of the progenitor SGMC is harder to estimate. As will be discussed further below, we postulate that the value of $\eta \equiv 10^{-3}\eta_3$ is likely to have been the same for SGMCs as for contemporary GMCs in the galaxy. This assumption implies that the progenitor SGMC cloud had a median mass $\bar{M}_{\rm SGMC} = 7.0 \times 10^8(\epsilon_f \eta_3)^{-1}\ M_\odot$, which is a factor of

$$\bar{m}_{\rm cloud} \simeq 2.0 \times 10^3(\epsilon_f \eta_3)^{-1} \quad (4.9b)$$

more massive than GMCs currently observed in the disk of our own Galaxy. The typical *maximum* mass of the SGMCs is then in the range $M_{\rm SGMC}({\rm max}) \simeq 3 \times 10^9(\epsilon_f \eta_3)^{-1}\ M_\odot$.

5. A VIRIAL MHD MODEL FOR SGMCS AND THEIR CORES

Most previous models of globular cluster formation have assumed that the protocluster clouds are *thermally* supported against gravity, so that considerable effort has gone into analyzing their cooling histories (e.g., Fall & Rees 1985; Shapiro & Kang 1987; Kang et al. 1990; Murray & Lin 1992, 1993). These analyses show that they would cool efficiently either by the formation of molecular hydrogen (for clouds with metallicities less than [Fe/H] $\lesssim -2$) or through heavy elements (for [Fe/H] $\gtrsim -2$). External sources of UV or X-ray flux (an active galactic nucleus, a background of hot halo gas, or an ambient population of massive "Population III" stars) have therefore been invoked to keep the clouds stable long enough to allow buildup to the necessary globular cluster mass range. However, each of these mechanisms has well known difficulties: Murray & Lin (1993) note that the background UV flux from hot halo gas would be insufficient to offset cooling for [Fe/H] $\gtrsim -2$ (which is the metallicity range that includes virtually all known globular clusters!). AGNs are also of doubtful utility, since in most galaxies they would be too weak or short-lived to keep even moderately metal-poor gas clouds from cooling rapidly. Similarly, an initial population of massive stars would have to last over at least 3 Gyr (see § 6.1 below) and be quite widespread through the halo.

In general, these external heating mechanisms should also depend rather sensitively on the size and/or type of the particular host galaxy involved. However, observations of globular clusters in many other galaxies (Harris 1991, 1993, and our Fig. 2) demonstrate that they formed with near-identical mass distributions in all galaxy types and over two orders of magnitude in metallicity, including many environments (such as the LMC or the dwarf ellipticals) in which *any* of these external heat sources can scarcely have been relevant. These data suggest that the protoglobular clouds require a more robust internal support mechanism that does not depend critically on the external environment.

5.1. *SGMCs and Clusters in the Milky Way: Estimates*

To develop a more specific model for SGMCs and their cores, we now assume explicitly that (1) the clouds and their cores are in virial balance, (2) they are primarily supported by internal magnetic pressure (both mean field and "turbulent"), and (3) the clouds are confined by self-gravity and a surface pressure P_s which is much larger than the pressure $P_{\rm ISM}$ of the host galaxy (Elmegreen 1989; see below). The cooling and heating of clouds by surrounding sources, as well as effects of differing metallicity, are of little relevance as long as the magnetic field is the primary form of support against gravitational collapse.

Adopting the virial relations

$$D \propto M^{1/2}\ ;\quad n \propto M^{-1/2}\ ;\quad \sigma_v \propto M^{1/4}\ .$$

for both the cores and the clouds, along with relations (4.9), we can now estimate the SGMC cloud properties for the proto-Milky Way. These are summarized in Table 3. The SGMCs are typically 45 times larger in diameter and have mean densities only 2% of typical contemporary Galactic GMCs; their velocity dispersion is ~ 7 times larger. The SGMCs that we postulate are clearly large enough and massive enough to qualify as the "fragments" from which the entire Milky Way Galaxy was built (Searle & Zinn 1978; Larson 1990, 1992, 1993). If the Milky Way protogalactic gas comprises $\sim 10^{11}\ M_\odot$ inside a radius $R_{\rm gc} \simeq 30$ kpc (where we take $R_{\rm gc}$ to be the observed extent of the normal halo as defined by the RR Lyrae stars and globular clusters; e.g., Harris 1976; Zinn 1985; Saha 1985), then the mean protogalactic gas density is of order $\langle n \rangle \simeq 3.6 \times 10^{-2}\ {\rm cm}^{-3}$, or $\sim 1\%$ that of the median SGMC.

Half of the entire SGMC mass spectrum is contained in $N_{\rm SMGC}(>50\%) = 20(\epsilon_f \eta_3)M_T$ clouds, where M_T is the total protogalactic gas mass in units of $10^{11}\ M_\odot$. In other words, a typical disk galaxy the size of the Milky Way may have been built out of only a couple of dozen large clouds (plus many more small ones; see Larson 1992 for a similar estimate). A giant elliptical would have required more than 1000 large clouds for the same intrinsic SGMC mass spectrum.

As noted above, the SGMC cloud *cores* are objects that we identify as protoglobular clusters. Their predicted properties are also given in Table 3. Here, we have explicitly *assumed* that the core mass fraction η has the value 10^{-3} derived in equation (3.1); this assumption is made without proof, though we will provide additional consistency arguments in favor of it in § 7 below. The ~ 15 pc size of the median core (from the virial relation $\bar{D}_{\rm core} = \bar{m}_{\rm core}^{1/2}\bar{D}_{\rm GMC,core}$) indicates that it was typically 40 times larger than, and had 3% of the density of, current GMC cores, but with internal velocity dispersions 6 times larger. More importantly, these mean core properties are in excellent accord with the mean densities, tidal radii, and internal velocity dispersions of typical halo globular clusters (e.g., Webbink 1985; Murray & Lin 1992).

5.2. *MHD Equilibria for Clouds and Cores*

Application of the virial theorem to magnetized molecular clouds shows that GMCs and their most massive cores are supported equally by a mean and turbulent magnetic field. These objects are near their critical mass which can be shown to consist of two contributions, $M \simeq M_{\rm cr} = M_\Phi + M_{\rm J}$ (McKee

TABLE 3

ESTIMATED MEDIAN CORE AND CLOUD PROPERTIES FOR GALACTIC SGMCS

Parameter	Median Core	Median Cloud
$\bar{M}\ (M_\odot)$	$8.4 \times 10^5\epsilon_f^{-1}$	$7.0 \times 10^8 v^{-1}$
$\bar{r}$ (pc)	$15\epsilon_f^{-0.5}$	$0.9 \times 10^3 v^{-0.5}$
$\bar{n}\ ({\rm cm}^{-3})$	$0.90 \times 10^3\epsilon_f^{0.5}$	$4.0v^{0.5}$
$\bar{\rho}\ (M_\odot\ {\rm pc}^{-3})$	$60\epsilon_f^{0.5}$	$0.23v^{0.5}$
$N\ (10^{22}\ {\rm cm}^{-2})$	6.5	1.4
$\Sigma\ (M_\odot\ {\rm pc}^{-2})$	1.2×10^3	260
$\bar{\sigma}_v\ ({\rm km\ s}^{-1})$	$6.9\epsilon_f^{-0.25}$	$25v^{-0.25}$

NOTE.—$v \equiv \epsilon_f \eta_3$.

1989; McKee et al. 1993). In this expression, $M_\Phi = 0.12\Phi/G^{1/2}$ is the critical mass for a cloud supported purely by a mean magnetic field whose magnetic flux through the cloud is $\Phi = \pi B r^2$ (where B is the cloud magnetic field strength and r is its radius); and M_J is the Jeans mass for a cloud supported by turbulence with a (one-dimensional) velocity dispersion σ. In practice, the waves or turbulence inferred to exist from the observed nonthermal line profiles in GMCs also provide a pressure support that is comparable to that for the mean magnetic field in the cloud, $M_\Phi \simeq M_J$. Thus the critical mass of the cloud is $M_{cr} \simeq 2M_J$.

Now consider an isothermal cloud with an internal one-dimensional velocity dispersion σ, mass M, radius r, and mean density $\rho \equiv M/(4\pi/3)r^3$. We assume the cloud to exist in an external medium that exerts a surface pressure P_s upon it. Similarly, cores embedded within clouds have a surface pressure exerted upon them owing to the pressure $P_{s,c}$ of the surrounding cloud. The equilibrium relations for pressure bounded, self-gravitating, isothermal spheres were first derived by Ebert (1955) and Bonnor (1956). These relations are generalized to hydromagnetic equilibria by Elmegreen (1989) (see also McKee et al. 1993). Following McKee et al., we express the virial theorem as

$$M = \frac{5}{\gamma}\frac{\sigma^2 r}{G}, \tag{5.1}$$

where all the effects of magnetic fields are taken up in the factor γ. It is straightforward to solve for the coefficients in the general virial relations in terms of γ. We can then derive generalized Ebert-Bonnor relations,

$$M = \frac{3.45}{\gamma^{3/2}}\frac{\sigma^4}{(G^3 P_s)^{1/2}}, \tag{5.2a}$$

$$r = \frac{0.69}{\gamma^{1/2}}\frac{\sigma^2}{(GP_s)^{1/2}}, \tag{5.2b}$$

$$\rho = 2.52\frac{P_s}{\sigma^2}, \tag{5.2c}$$

$$t_{ff} = 0.342\frac{\sigma}{(GP_s)^{1/2}}. \tag{5.2d}$$

The density-size and linewidth-size relations that follow from these take the form

$$\Sigma = \frac{M}{\pi r^2} = \frac{2.32}{\gamma^{1/2}}\left(\frac{P_s}{G}\right)^{1/2}, \tag{5.3a}$$

$$\frac{\sigma}{r^{1/2}} = 1.21\gamma^{1/4}(GP_s)^{1/4}. \tag{5.3b}$$

Elmegreen (1989) noted that the two important relations $\Sigma \simeq$ const and $\sigma \propto r^{1/2}$ follow from equation (5.3) if the surface pressures P_s are all about the same. The same principle pertains to the more massive cores as well, except that these must of course be at higher surface pressure than the clouds. As Elmegreen emphasizes, the source of the velocity dispersion itself is irrelevant; clouds in virial equilibrium adjust their radius and density so that their boundary has the pressure of the environment.

The surface pressure on cloud complexes is substantially greater than that of the hot surrounding ISM because complexes are embedded in dense H I envelopes, and typically $P_s \simeq 5P_{ISM}$ (Elmegreen 1989). In what follows, we shall adopt a typical surface pressure on the median GMC in the Milky Way of

$$\bar{P}_s = 10P_{ISM} \simeq 2 \times 10^5 k \text{ cm}^{-3} \text{ K}, \tag{5.4}$$

where k is Boltzmann's constant. The Ebert-Bonnor equilibria are recovered by setting $\gamma = 2.04$, for which value $M = M_J$ in equation (5.2a). In this case, the one-dimensional velocity dispersion of the gas in $\sigma = (kT/\mu m_p)^{1/2}$. The resulting relations were used by Fall & Rees (1985) in their model of thermally supported equilibria.

Magnetized equilibria, for which $M \simeq 2M_\Phi$, are obtained by setting $\gamma \simeq 1$ (McKee et al. 1993). In this case, the one-dimensional velocity dispersion is due primarily to Alfvén waves or Alfvénic "turbulence." The Alfvén wave speed is just the natural transverse wavespeed along the field. Thus, the amplitude of the nonthermal one-dimensional motions in such clouds is

$$\sigma = V_A/\sqrt{3} \equiv (1/\sqrt{3})B/(4\pi\rho)^{1/2}. \tag{5.5}$$

The critical magnetic field strength B_c needed to support a cloud of given column density against collapse is then

$$B_{crit} = 5.1(M/M_\Phi)^{-1}N_{21}\,\mu\text{G}, \tag{5.6}$$

where M is the cloud mass and N_{21} is its surface density in units of 10^{21} cm^{-2}, and $M/M_\Phi = 2$. For our typical SGMCs whose column densities we have calculated above, we find $B_{crit} \simeq 43\,\mu$G.

We may reduce the relations (5.2) and (5.3) to more useful form now by setting $\gamma = 1$ and expressing the various physical quantities in terms of the cloud or core radius. The variable parameter is the surface pressure. The surface density of clouds is

$$\Sigma_{cl} = 228(P_s/2 \times 10^5)^{1/2}\, M_\odot \text{ pc}^{-2}, \tag{5.7}$$

where cloud radii are measured in parsecs, and surface pressures in k cm^{-3} K. The remaining relations are

$$\begin{aligned} M_{cl} &= 712(P_s/2 \times 10^5)^{1/2} r_{pc}^2\, M_\odot, \\ \rho_{cl} &= 168(P_s/2 \times 10^5)^{1/2} r_{pc}^{-1}\, M_\odot \text{ pc}^{-3}, \\ \sigma_{cl} &= 0.78(P_s/2 \times 10^5)^{1/4} r_{pc}^{1/2} \text{ km s}^{-1}. \end{aligned} \tag{5.8}$$

It is straightforward to derive the analogous virial formulae for the cores within clouds. From equation (5.2) we see that the ratio of the core to cloud surface density depends only upon the core and cloud surface pressures, $\Sigma_{co}/\Sigma_{cl} = (P_{co}/P_{cl})^{1/2} \equiv \not{\mu}$. Using the Galactic GMC data as a guide, we take $\not{\mu} = 4.64$. Then the relations for cores follow from those in equation (5.8): $M_{co} = \not{\mu} M_{cl}$, $\rho_{co} = \not{\mu}\rho_{cl}$, and $\sigma_{co} = \not{\mu}^{1/2}\sigma_{cl}$, for a given radius r.

We plot the results (5.8) for both the clouds and the cores in Figure 5 (mass vs. radius; the other quantities including density and velocity dispersion can be readily calculated from the above relations). In each graph, we show model lines corresponding to a four-decade range in pressure P_s. In Figure 5*a*, we suggest that the low end of the P_s scale might be applicable to very low mass, low-density galaxies, or the outer parts ($R \geq 30$ kpc) of galactic haloes; the middle range may typify the surface pressures of clouds at $\sim$10 kpc in spiral galaxies; while the upper end may typify the pressures exerted on SMGCs in the Galactic bulge, or in very dense, massive elliptical galaxies. The median Milky Way GMC (Table 2) lies near the lower left part of Figure 5*a*; our proposed SGMCs which

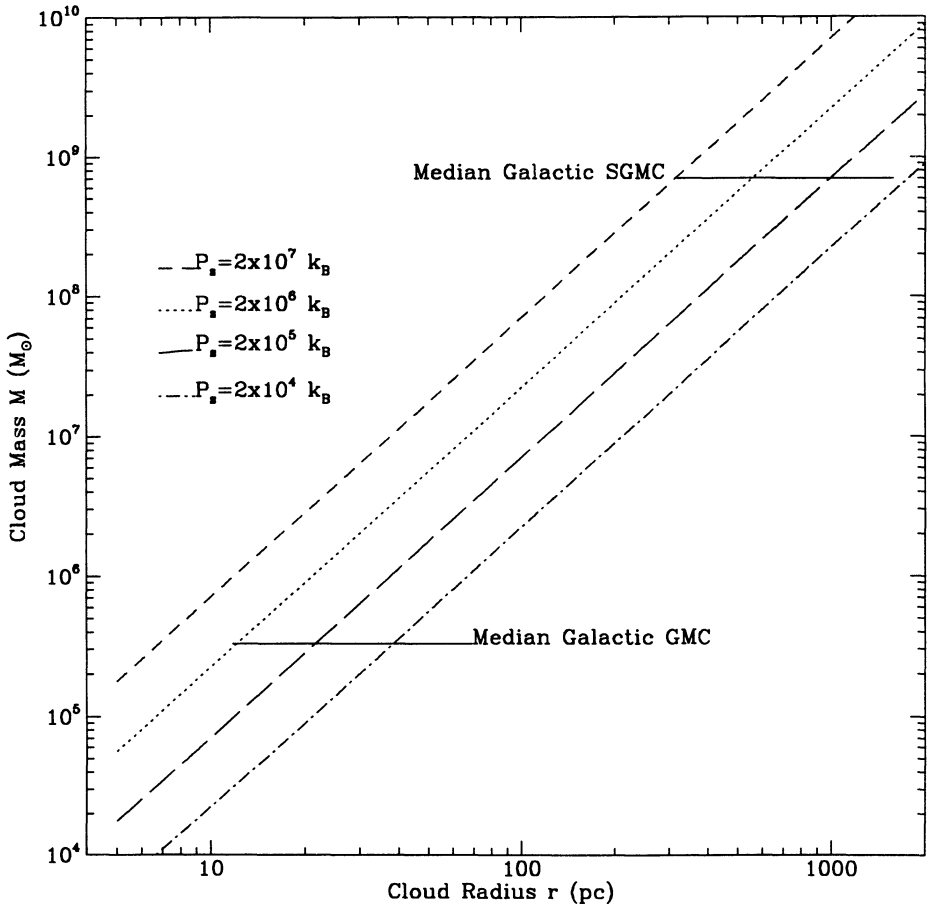

FIG. 5a

FIG. 5.—Masses of clouds (*a*) and cores (*b*) as a function of cloud (or core) radius r, as given by eq. (5.8) in the text. The log-log plots extend over the range of radii for both GMCs and SGMCs. Four different values for the surface pressure on clouds are shown as the straight lines, where (*from top to bottom*) $(P_s/k_B) = 2 \times 10^7$, 10^6, 10^5, 10^4, and k_B is Boltzmann's constant. The cores are taken to have surface pressures a factor of $\phi = 4.6$ times larger than the cloud surface pressures (see text). In panel (*b*), the *present-day* values for mass M and half-mass radius r_h for globular clusters in the Milky Way halo (van den Bergh et al. 1991) are plotted for comparison, as are the values for observed cluster cores in the Orion GMC. The globular clusters are subdivided into three ranges of galactocentric distance R: *crosses* denote the inner clusters ($R < 6$ kpc), *open circles* clusters in the middle halo (6–40 kpc), and *solid circles* the outermost Palomar-type clusters. Typical surface pressures $P_s = 10^{6\pm1} k_B$ on the cloud cores appear to provide a satisfactory match to the protoglobular clusters as well as contemporary cluster cores.

are the sites of massive globular cluster formation must lie much farther up on these lines (Table 3).

In the second panel of Figure 5 we also plot (at lower left) the effective radii and masses for the five largest cluster-containing cores in the Lynds 1630 molecular cloud in Orion B (Lada et al. 1991), for which the data are particularly well defined. For comparison, at upper right are the *present-day* globular clusters in the Milky Way (van den Bergh, Morbey, & Pazder 1991). Note that the quantity plotted for each globular cluster is the half-mass radius r_h, which is nearly unaffected by dynamical evolution after cluster formation. Although the *protocluster* core radius should be larger by a factor of ~ 2 (cf. Murray & Lin 1992), the protocluster mass should also be larger than the cluster today by roughly the same factor after accounting for dynamically driven mass loss over 10^{10} yr (e.g., Aguilar et al. 1988; Chernoff & Weinberg 1990; Lee et al. 1991; Johnstone 1993). Thus in Figure 5*b*, to recover the characteristic quantities of the protoclusters we should move each point upward roughly parallel to the model lines, preserving the overall fit. We conclude that the range of model surface pressures P_s represented in the figure is consistent with our predicted properties for the SGMC cores.

5.3. *SGMC Lifetimes and the Epoch of Cluster Formation*

As mentioned earlier, the relation (4.2) allows us to estimate the lifetime of the SGMCs and hence place limits on the epoch of globular cluster formation, presuming that they were the first stellar systems to form in the protogalaxies. Rewriting relation (4.2) in terms of the cloud lifetime τ, and noting $\sigma_M \propto M$, we find that it takes the same form for any mass. Thus, it is convenient to evaluate it for the median cloud, i.e., $\tau = \bar{M}/(\beta\rho\sigma_M v_0)$. Now, since the collision cross sections of clouds are geometric, then $\bar{M}/\bar{\sigma}_M = \bar{\Sigma}_M$. Furthermore, since the surface densities of clouds are the same regardless of their mass, we can then take $\bar{\Sigma}_M \simeq \Sigma_{\rm SGMC}$. Thus, our expression for the cloud lifetime simply reduces to

$$\tau = \frac{\Sigma_{\rm SGMC}}{\beta\langle\rho\rangle v_0} = \frac{1.31 \times 10^9}{\beta} \frac{(R_{\rm gc}/30\ {\rm kpc})^3}{M_T} \frac{(220\ {\rm km\ s^{-1}})}{v_0}\ {\rm yr}\ , \tag{5.9}$$

where we have taken v_0 to be of order the circular speed in the dark matter potential well of the protogalaxy. For a value of $\beta = 2.2$, we find that the lifetime of SGMCs in the Milky Way should have been $\tau \simeq 6.0 \times 10^8$ yr.

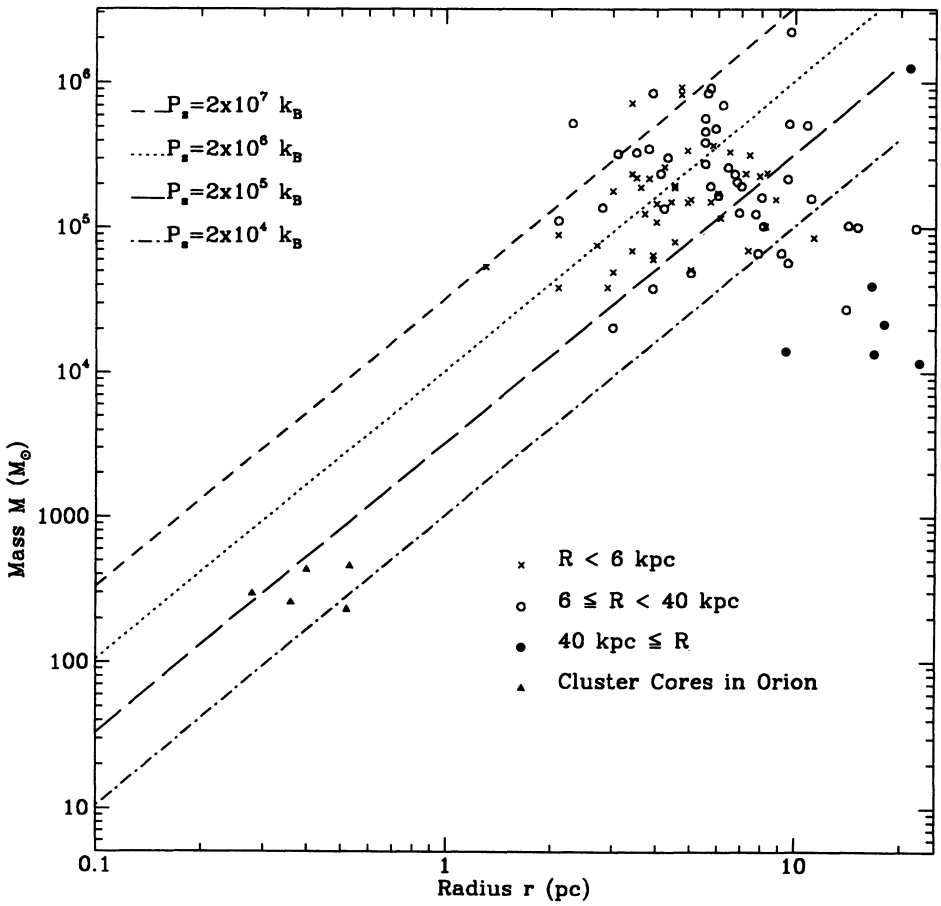

FIG. 5*b*

We may now reasonably predict the redshift at which the globular clusters may have started to appear, i.e., the epoch at which the SGMCs began star formation. For a standard inflationary cosmology with $\Omega_0 = 1$, $\Lambda = 0$, and $H_0 = 50$ km s^{-1} Mpc^{-1}, the time $\tau = 6 \times 10^8$ yr corresponds to $z \simeq 8$; for $\Omega \simeq 0.2$ and $H_0 = 75$, we have $z \simeq 9$. These are extreme upper limits to z(SGMC); if we allow (say) an initial $\sim$0.5 Gyr to pass before the dark-matter potential wells of the protogalaxies are set up and the SGMC's begin forming, then their globular clusters would emerge at $z \lesssim 5$. These redshifts are in accord with other arguments for the timescale at which galactic halos form; for the most massive galaxies such as giant ellipticals, this epoch was well underway by $z \sim 3$ and must have started before $z \gtrsim 5$ (e.g., Cowie 1988; Lilly 1988; cf. also the models of Katz 1992). Since the globular cluster systems in large galaxies are more metal poor and more spatially extended than the halo itself (Harris 1991), we expect that the globular clusters would have formed slightly earlier than the bulk of the halo (though perhaps not as early as the innermost bulge, where the gas density was highest and chemical enrichment would have proceeded fastest; cf. Lee 1992a).

The free-fall collapse time of the magnetically supported clouds is

$$\bar{t}_{\rm ff,cl} \equiv (3\pi/32G\bar{\rho})^{1/2} = 6.31 \times 10^5 (P_s/2 \times 10^5)^{-1/4} r_{\rm pc}^{1/2} \text{ yr} . \quad (5.10)$$

While the median GMC has $\bar{t}_{\rm ff,GMC} = 2.82 \times 10^6$ yr our *SGMCs have much longer dynamical timescales* $\bar{t}_{\rm ff,SGMC} = 1.89 \times 10^7$ yr for the same surface pressures, because SGMCs are nearly 100 times less dense than contemporary GMCs.

It is strongly suspected that GMCs must live many free-fall times, because star formation within clouds must continue for many Myr. An excellent candidate for supporting GMCs this long is, again, the large-scale magnetic field and Alfvénic turbulence (cf. Richer et al. 1993 for additional discussion of this view, in the context of cluster formation from the massive amounts of infalling gas within the nuclear region of NGC 1275). The supporting magnetic field leaks away very slowly by ambipolar diffusion. Many calculations predict that $t_{\rm AD} \sim 10 t_{\rm ff}$, independent of the gas density (e.g., Carlberg & Pudritz 1990; McKee et al. 1993), so that magnetic support will maintain the SGMCs for a time of order 2×10^8 yr.

As the field strength drops, the cloud and especially the cores become very dense, and the main phase of star formation then proceeds in earnest. Thus, we anticipate that when $\tau \simeq 3t_{\rm AD}$, globular cluster formation in the cores has become so well established and has led to so much supernova activity that a good fraction of the clouds has been disrupted (as well as chemically enriched). The SGMC gas can then collapse dissipatively further in the dark-matter potential well of their protogalaxy, and begin the main phase of halo star formation. This provides a basic physical explanation for the value of our

timescale τ. In addition, it provides a natural route for generating the higher spatial concentration and higher metallicity of the halos of giant galaxies compared with their globular cluster systems.

Our simple theory clearly requires that dynamically significant magnetic fields existed throughout protogalactic halos at early times. The SGMC fields are amplified by the compression of the magnetized gas of the early galactic ISMs. The expected scaling of magnetic field with the gas density in the galaxy is $B \propto \rho^{2/3}$ (see below). Thus a field of $B \simeq 2$ μG threading the ISM of protogalactic halos can be amplified to $\bar{B}_{\rm SGMC} \simeq 40$ μG by compression within the denser median SGMC, in agreement with the critical field strength calculated above. There is some direct evidence for microgauss-sized fields in younger galaxies (see Welter, Perry, & Kronberg 1984 for relevant data). Magnetic field generation in the ISM of protogalactic halos could occur during the dissipative collapse of gas that occurred in earlier epochs than we are considering here (Pudritz & Silk 1989; Pudritz 1990).

6. CHARACTERISTICS OF GLOBULAR CLUSTER SYSTEMS

In summary, our model proposes that globular cluster systems originate in the collection of SGMCs that inhabit galactic potential wells at early times. Each of the SGMCs manufactures a replica in miniature of the overall globular cluster mass spectrum. As long as this process is governed by the virial equilibrium rules then it is possible to account fairly simply for the observed near-universality of the cluster mass distribution among a wide range of galaxies. There are, however, several other observable features of globular cluster systems that also find natural explanations in this model. We discuss these in the following sections.

6.1. *Metallicity and Age Spread*

In the Milky halo, considerable direct evidence now exists that the normal globular clusters and the field RR Lyrae stars possess an age range of $\Delta\tau \gtrsim 3$ Gyr (VandenBerg, Bolte, & Stetson 1990; Sarajedini & King 1989; Lee 1992b). In addition, within large galaxies the globular clusters exhibit a very significant cluster-to-cluster metallicity spread at all points in the halo, with typical dispersion σ[Fe/H] $\simeq$ 0.3–0.6. This variance in the metallicity distribution function (MDF) is distinctly larger than any overall gradient in *mean* metallicity through the halo, which is quite modest in the galaxies observed to date (e.g., Zinn 1985; Harris 1991; Ostrov, Geisler, & Forte 1993). These observations are well known to fit naturally within the basic Searle-Zinn formation picture in which the galaxy assembled by large fragments which may have built up the halo over several Gyr.

An important consequence of the Alfvénic turbulence within the protoglobular cloud cores, coupled with their long stable lifetimes, is that they will end up well mixed and therefore chemically homogeneous after star formation (Murray & Lin 1992). Except for a few of the very most massive globular clusters such as ω Cen or M22, observational constaints on the internal metallicity dispersion are extremely tight (σ[Fe/H] $\lesssim$ 0.05; cf. Suntzeff 1993) and thus require thorough mixing of just this type. At the same time, the cluster-to-cluster variance in metallicity can be considerably larger, depending on the exact amount of supernova preenrichment that took place within each SGMC both in and out of the protocluster cores (cf. Searle & Zinn 1978; Brown, Burkert, & Truran 1991; Larson 1992, for more extensive discussion). Thus in our model it is expected that each cluster should be *internally* very homogeneous, while each SGMC could undergo its own chemical evolution independently of the others and thus generate the large dispersion in the MDF.

In addition, the expectation that the clusters formed rather early within the SGMCs would allow them to preenrich the SGMC field star formation and thus create the observed metallicity offset between globular clusters and halo stars (cf. De Young, Lind, & Strom 1983; Brodie & Huchra 1991). This process would have continued until all the fragments were disrupted by collision and star formation, and their contents spilled into the general field of the halo. Recently Zinn (1993a) and van den Bergh (1993) have presented evidence that the traces of particularly large "fragments" (perhaps small protogalaxies in their own right) can still be seen in the kinematics of the Milky Way halo clusters.

In our model, a constant fraction of the SGMCs are disrupted every $\tau \simeq 1.5/\beta$ Gyr. Thus the observed values of β and $\Delta\tau$ would have allowed just a few generations of clouds to run through star formation and progressive metallicity enrichment before the SGMC epoch shut down.

6.2. *Dependence of Cluster Parameters on Galactocentric Radius*

All the scalings of cloud and core properties discussed to this point in our model assume that we are at a fixed galactocentric radius R. However, one of the most remarkable systematic relations for the Milky Way clusters is that their characteristic *diameters* increase with Galactocentric radius R, whereas their mean *masses* remain nearly uniform with R. This scaling law is demonstrated definitively by van den Bergh et al. (1991), who show that the cluster half-mass diameters D_h (which are nearly immune to internal dynamical evolution) increase as $D_h \propto R^{1/2}$, though with considerable scatter around the mean relation. The much weaker dependence of cluster mass on R is illustrated here in Figure 6, in which we have taken the data for the Milky Way and M31 clusters described in § 2 and replotted them in bins of galactocentric distance. Within the "normal" halo boundary $R \sim 30$ kpc, no significant trend of mean cluster luminosity is seen in either galaxy.

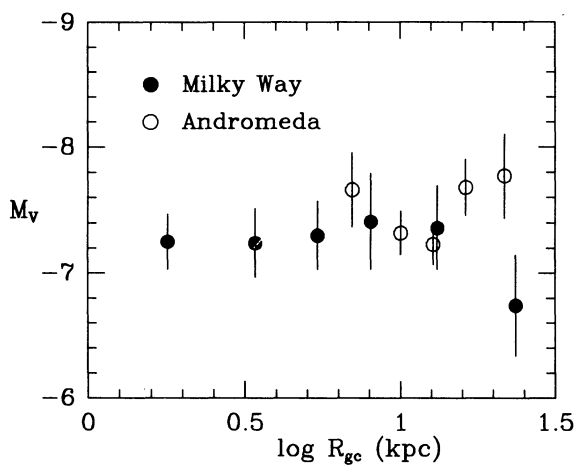

FIG. 6.—Mean absolute magnitudes $\langle M_V \rangle$ of the globular clusters in the Milky Way and M31, as a function of galactocentric distance. The data for the individual clusters are the same as used in Fig. 1 and § 2 of the text. Each plotted bin contains 15–20 clusters. For $R_{gc} \lesssim 30$ kpc, no dependence of mean luminosity on location is seen.

We propose that the van den Bergh et al. size-radius relations arises naturally if the SGMCs and protoclusters form within a hot, pressure-supported halo gas. The ISMs in the haloes of the protogalaxies will be in hydrostatic balance with their dark matter potential wells, which implies that typical diffuse ISM temperatures will lie in the X-ray regime (e.g., Farbicant, Lecar, & Gorenstein 1980; Cowie, Henriksen, & Mushotzky 1987). The pressure is well described by the relation

$$P_{\rm ISM} = P_0[1 + (R/a)^2]^{-3\phi/2} , \qquad (6.1)$$

where a is the core radius for the potential well. The index ϕ can be determined if the X-ray surface brightness of the halo can be fitted as a function of radius. Current *ROSAT* observations show that the gas in galactic potential wells is isothermal, with the best current value for ϕ being near 0.6. As discussed above, we also take the surface pressure of the SGMCs to be proportional to the surrounding gas pressure, $P_s \simeq 5$–$10 P_{\rm ISM}$. Thus for the halo region $R > a$, we have the scaling relation $P_s \propto R^{-2}$ to a good approximation. Then from equations (5.2) and *independent of the details on how SGMCs and cores are stirred*, we have $M \propto \sigma^4 R$ and $r \propto \sigma^2 R$. Since the protocluster cores follow the same relations as their parent clouds except for a normalizing factor $\not{\mu}$, the same scaling with radius pertains to cores as well. Finally, once we add in the *observational constraint* $M(R) \simeq$ const (Fig. 6), we obtain

$$\sigma \propto R^{-1/4} , \quad r \propto R^{1/2} . \qquad (6.2)$$

The latter relation is precisely the observed van den Bergh et al. (1991) scaling law. While it is not evident why cloud and cluster masses are independent of R, it is interesting to note that $M = 2M_\Phi \propto \Phi$ for virialized magnetic clouds. We speculate that this constancy may then be a simple consequence of the conservation of magnetic flux.

It follows from the above that the mass densities of clusters should follow

$$\rho(R) \propto R^{-3/2} . \qquad (6.3)$$

This is a more gently falling density law that might be expected for tidally limited clouds, for which $\rho \propto R^{-2}$ (see below). However, it agrees with the sense of GMC data, in which GMCs have densities typically 5 times larger than what arises from tidal limitation arguments (e.g., Scoville & Sanders 1987). Indeed, Surdin (1979), Fall & Rees (1977, 1985), and Murray & Lin (1992) show that globular cluster densities also exceed the tidal limits.

Last, we note that the surface density and magnetic field in SGMCs and cores scale as

$$\Sigma \propto B \propto R^{-1} , \qquad (6.4)$$

which combined with equation (6.3) predicts that

$$B \propto \rho^{2/3} \qquad (6.5)$$

This is the expected relation between density and magnetic field for a self-gravitating cloud undergoing isotropic contraction.

6.3. *Space Distribution in the Central Regions*

Globular cluster systems in large galaxies show deficiencies in the cluster population relative to the spheroid light in the innermost few kiloparsecs; that is, the projected spatial distribution levels off strongly in toward the galactic nucleus (see Harris 1991 for a review). As previously mentioned, there are several excellent potential explanations for this effect through the action of dynamical friction and tidal shocking by the bulge on any clusters whose orbits might penetrate in that far. However, an additional effect acting against the *formation* of such clusters is that our SGMCs would be torn up by tides. Within a given galaxy in equilibrium, the critical density for the tidal disruption of gas with mean molecular weight of 2.3 is

$$n_{\rm tide} = 78(V_m/220 \text{ km s}^{-1})^2 R_{\rm kpc}^{-2} \text{ cm}^{-3} , \qquad (6.6)$$

where V_m is the circular speed of the gas in the dark matter potential well of the galaxy, and R(kpc) is the galactocentric radius (see Fall & Rees 1985). Comparing this expression with the mean density of our median cloud, we find that median clouds would be torn apart inside a radius of $R \leq 4$ kpc.

The preceding estimate must be viewed as only an *upper limit* on the disruptive effects of tides, since in our picture the SGMCs would already have been producing star clusters before the protogalactic collapse stage had finished and thus before the Galactic tidal field was as strong as it is today. In fact, an interesting clue to the epoch at which the basic structure of the Galactic halo was complete may be contained in the cluster age distribution. The "classic" globular clusters have a modest age spread of $\lesssim 3$ Gyr, with a mean age of ~ 15 Gyr, according to current calibrations (e.g., VandenBerg et al. 1990). But a handful of halo clusters have recently been found that have ages in the range ~ 10–12 Gyr, i.e., clearly between the age of the normal halo and the oldest parts of the Galactic disk. These are objects such as Palomar 12 (Stetson et al. 1989; Gratton & Ortalani 1989) and Ruprecht 106 (Buonanno et al. 1993), and two or three others (Buonanno 1993). It is noteworthy that these anomalous globular clusters have a mean luminosity $M_V \simeq -5.3$, corresponding to $\bar{M} \simeq 2.3 \times 10^4\ M_\odot$. That is, they are on average almost *one order of magnitude less massive than the normal globular clusters.* This is just what would be expected if the original SGMCs had been tidally torn apart by that time, into smaller GMCs within which the star clusters being formed would be inevitably less massive.

6.4. *Specific Frequencies*

The core mass fraction η is related in an obvious way to the well known *specific frequency* S_N, the number of globular clusters per unit galaxy luminosity (Harris & van den Bergh 1981). If M_V^T is the absolute magnitude of the galaxy and N_T is its total globular cluster population, then the specific frequency by number is defined as $S_N = N_T \times 10^{0.4(15 + M_V^T)}$. Rewritten in terms of the V-band galaxy luminosity L_T, this becomes

$$S_N \simeq 8.6 \times 10^7\ L_\odot\ N_T/L_T . \qquad (6.7)$$

To connect S_N with η, first we define a specific *mass* ratio $S_M \equiv M_{\oplus,T}/M_{g,T}$ equal to the fraction of the galaxy's stellar mass in the globular clusters. But now, $M_{\oplus,T}$ must equal $\delta\epsilon \cdot M_{{\rm core},T}$, where $M_{{\rm core},T}$ is the total gas mass in the protocluster cores; ϵ is the star formation efficiency as before; and δ is the fraction of the initial cluster mass still left today after the destructive effects of tidal stripping, evaporation, etc. Both ϵ and δ are uncertain to within factors of ~ 2 (cf. the references cited in § 5.2 for recent discussions of mass-loss rates), but using the estimates quoted above we adopt $\epsilon\delta \simeq 0.3$. In a large galaxy, the total protostellar gas mass will fairly quickly all be turned into stars, so we have $M_{{\rm core},T}/M_{g,T} = (\eta c)$, where c is the average number of protocluster cores per SGMC and η, as before, is the core-to-SGMC mass ratio. Combining these

factors leads to $S_M = \delta\epsilon\eta c \simeq 0.3\eta c$ for the specific mass fraction.

Before we relate S_M to S_N, we transform it into the more directly observable *specific luminosity* $S_L = L_{\oplus,T}/L_T$ (Harris 1991), where L_T is the total light in the entire galaxy's old stellar population and $L_{\oplus,T}$ is the total light in the clusters. If the mean mass-to-light ratio for the clusters is $(M/L)_{\oplus,V} \simeq 2$ and for the old-spheroid stellar population is $(M/L)_{T,V} \simeq 8$ (Faber & Gallagher 1979), then we have $S_L \simeq 4S_M$. As the final translation step, we rewrite equation (6.7) as

$$S_N = 8.6 \times 10^7 \, L_\odot \, S_L \left(\frac{N_T}{M_T}\right)\left(\frac{M}{L}\right)_\oplus \qquad (6.8)$$

and then use relations (4.4) and (4.5) to evaluate (N_T/M_T). With our fiducial values for α, α_2, $M_{\max}$, the mass-to-light ratio $(M/L)_\oplus = 2$, and $S_L = 4S_M$, we finally obtain $S_N \simeq 350S_L \simeq 1400S_M$, or $S_N \simeq 0.4\eta_3 c$ in terms of the core mass fraction.

In normal galaxies, *observed* global specific frequencies run from $S_N \simeq 2$ up to ~ 20 (Harris 1991). For the spheroids of the Milky Way, M31, and other disk galaxies, we find $\bar{S}_N \simeq 2$, which yields $\eta_3 c \simeq 5$. This ratio is remarkably consistent with the order-of-magnitude core mass fraction $\eta_3 \sim 1$ proposed previously in § 3, as long as it is reasonable to expect each SGMC to form a handful of protocluster cores (i.e., c would need to be of order 5; again, this is quite consistent with what we observe in contemporary GMCs such as the Orion B molecular cloud, where five of the most massive cores are producing identifiable star clusters; see Lada et al. 1991). However, spiral galaxies are at the low end of the S_N scale. At the opposite extreme, for the very rich globular cluster systems in M87 and many other central giant cD galaxies, we have $\bar{S}_N \simeq 15$ and thus $\eta_3 c \sim 50$. These galaxies somehow generated clusters with far higher efficiency.

The strong observational constraints on the similarity of the GCLF in different galaxies tell us that the protocluster cores themselves must have had very much the same masses in all galaxy environments. Thus in our model, we are left with only two available routes to explain the wide observed range in specific frequencies: the high-S_N galaxies must either have formed from larger numbers of proportionately smaller SGMCs (thus requiring a higher mass ratio η_3); or each SGMC must have generated more protoclusters (thus requiring a higher number ratio c).

Although we have no unambiguous evidence to support one alternative over the other, we suggest that the latter approach (more efficient generation of protocluster cores within SGMCs of about the same size) is likely to be the solution. For example, giant galaxies located at the centers of rich clusters are the only sites where extremely high-S_N systems are found; cf. Harris, Pritchet, & McClure (1993). The high ISM pressures necessarily attained in these very massive protohalos would lead to higher overall SGMC surface densities. This implies that a higher fraction of the gas in these clouds should be dense enough to produce cluster forming cores. (See also West 1993 for a similar solution based on a "biasing" approach to protocluster formation.) Observational support for such a conjecture comes with the recent finding that molecular clouds in the bulges of galaxies have twice the amount of dense, HCN-emitting gas as do GMCs in the disks of such galaxies (Helfer & Blitz 1993; Spergel & Blitz 1992).

7. DWARF GALAXIES

The fate of contemporary GMCs is fairly well understood: massive star formation with OB-star ionizing flux and supernova production has energetic enough consequences to entirely disrupt them, and the clusters that have formed in their cores are then released into the Galactic disk, to subsequently begin their lives as stellar associations of various types. The unused but metal-enriched gas of the GMC is dispersed and rejoins the interstellar medium.

There are two possible fates of SGMCs after massive star formation and cluster formation have occurred. Since these systems are so much more massive than contemporary GMCs, they can more easily resist dispersal by modest rates of massive star formation. If disrupted externally by collisions, they would spill their young globular clusters out into the galactic halo. The unused but metal-enriched gas would then settle dissipatively into the gravitational potential well of the dark-matter halo, building up a higher central concentration and acting as the reservoir for future halo star formation.

Any SGMCs that remain bound and survive outside the potential wells should, however, evolve into something resembling dwarf galaxies (see Larson [1992, 1993] for an extensive review on the role of these objects). The predicted mass range of our SGMCs (up to $\sim 3 \times 10^9 \, M_\odot$ in spiral galaxies) is easily large enough that, *if left in isolation*, any one of them would evolve into a dwarf galaxy with a small retinue of globular clusters. If the residual gas is stripped away at some later time, the remaining body would resemble the dE and dwarf spheroidal galaxies that are found in large numbers around bigger galaxies (Freeman 1993). Given the many hundreds of SGMCs that would be required to construct a giant E galaxy, we suggest that the dozens of dE, N dwarfs that are observed in the Virgo and Fornax Clusters (Sandage & Bingelli 1984; Ferguson 1989; Ferguson & Sandage 1991) might well be unused pieces from the formation of the big ellipticals there.

For the Local Group galaxies and similarly sparse environments where isolated SGMCs could hold on to their internal supply of gas, a wider variety of dwarf systems could result. Zinn (1980, 1993b) has assembled considerable evidence from stellar population analysis that the dwarf spheroidal galaxies and even the dwarf irregulars can reasonably be regarded also as leftover "building blocks." All the dwarf galaxies in the Local Group have masses within our predicted SGMC range (the LMC itself approaches the upper end of the SGMC mass spectrum), and thus each one might plausibly have evolved from a single initial fragment. A hint of what a typical SGMC might have looked like in its early stages is, perhaps, provided by present-day objects like the DDO 154 dwarf studied by Carignan & Freeman (1988); this small irregular has a baryonic mass of a few $10^8 \, M_\odot$ and has not yet gone through its main star formation epoch since most of it is still gaseous. Other examples listed by Larson (1992) include the blue compact dwarfs I Zw 18 and NGC 1705.

8. SUMMARY

We have developed a model for the formation of globular cluster systems based on the properties of self-gravitating, magnetized, and pressure-confined clouds. These properties fit the observations of present day GMCs and their cluster-forming cores. We extend this theory to consider SGMCs massive enough to contain cores of the order of globular cluster masses, with the following results:

1. The globular clusters in large disk galaxies, normal large ellipticals, and cD's all follow a near-universal mass distribution characterized by a simple power law with mass spectral index $\alpha \simeq 1.6$–1.7 for $M \lesssim 3 \times 10^6 \, M_\odot$. This distribution is

basically smilar to that found in contemporary sites of cluster formation such as GMCs and giant H II regions and can be accurately reproduced on theoretical grounds by a simple model of cloud growth by agglomeration.

2. If globular clusters formed in the same way as young star clusters today, then for spiral galaxies, the SGMCs containing them must have had typical masses approaching $10^9\ M_\odot$ and 1 kpc diameters; these large clouds are therefore appropriate candidates for the Searle-Zinn fragments from which the Milky Way is believed to have assembled. If left in isolation, a given SGMC should evolve into an object strongly resembling a dwarf galaxy. For giant E galaxies, on the other hand, the SGMCs produce cores and globular clusters of the same mass, but either (*a*) the SGMCs themselves were systematically less massive by factors of 3–10, or (*b*) each SGMC produced cluster core more efficiently by the same factor.

3. Protocluster clouds can be supported against gravitational collapse by magnetic field pressure and Alfvénic turbulence (as they are for contemporary molecular clouds), for time intervals $\sim 10\tau_{\rm ff}$ sufficiently long for growth up to the necessary masses. The field strength within the typical SGMCs needs to be of order $B \sim 40\ \mu$G. This mechanism relies only on the internal characteristics of the SGMC's and not on arbitrary external sources of UV flux (AGNs, massive first-generation stars, etc.), thus permitting the basic similarity of globular clusters across all types of galaxies to be readily predicted.

4. The growth time of the clouds can be estimated from the slope of the upper end of the mass spectrum ($N \sim M^{-3.2}$), and gives $\tau \sim 0.6$ Gyr. The oldest globular clusters in large galaxies should then have started to appear no earlier than a redshift $z \simeq 8$, and more realistically $z \simeq 5$.

5. The systematic increase of globular cluster scale size with Galactocentric radius ($r_h \sim R^{1/2}$) arises naturally if SGMCs are self-gravitating clouds that are also pressure confined by the host ISM within the dark matter potential well of the host galaxy.

We are indebted to K. Ashman, R. Larson, T. Richtler, V. Surdin, P. Sutherland, C. Wilson, and an anonymous referee for stimulating comments and advice. R. E. P. thanks the kind hospitality of C. Bertout and the staff of the Laboratorie d'Astrophysique at the Observatorie de Grenoble, as well as that of P. Myers and the Harvard-Smithsonian division of Radio and Geoastronomy, where much of this work was carried out during a research leave. This research was supported by the Natural Sciences and Engineering Research Council of Canada through operating grants to the authors.

REFERENCES

Aguilar, L., Hut, P., & Ostriker, J. P. 1988, ApJ, 335, 720
Armandroff, T. E. 1989, AJ, 97, 375
Ashman, K. M., & Zepf, S. E. 1992, ApJ, 384, 50
Bally, J., Langer, W. D., Stark, A. A., & Wilson, R. W. 1987, ApJ, 312, L45
Blitz, L. 1991, in The Physics of Star Formation and Early Stellar Evolution, ed. C. J. Lada & N. D. Kylafis (Dordrecht: Kluwer), 3
Bonnor, W. B. 1956, MNRAS, 116, 351
Bridges, T. J., & Hanes, D. A. 1992, AJ, 103, 800
Bridges, T. J., Hanes, D. A., & Harris, W. E. 1991, AJ, 101, 469
Brodie, J. P., & Huchra, J. P. 1991, ApJ, 379, 157
Brown, J. H., Burkert, A., & Truran, J. W. 1991, ApJ, 376, 115
Buonanno, R. 1993, in ASP Conf. Ser. 48, The Globular–Galaxy Connection, ed. G. Smith & J. Brodie (San Francisco: ASP), 131
Buonanno, R., Corsi, C., Fusi Pecci, F., Richer, H. B., & Fahlman, G. G. 1993, AJ, 105, 184
Carignan, C., & Freeman, K. C. 1988, ApJ, 332, L33
Carlberg, R. G., & Pudritz, R. E. 1990, MNRAS, 247, 353
Castets, A., Duvert, G., Dutrey, A., Bally, J., Langer, W. D., & Wilson, R. W. 1990, A&A, 334, 469
Chernoff, D. F., & Weinberg, M. D. 1990, ApJ, 351, 121
Cowie, L. L. 1988, in The Post Recombination Universe, ed. N. Kaiser & A. N. Lasenby (Dordrecht: Kluwer), 1
Cowie, L. L., Henricksen, M., & Mushotzky, R. 1987, ApJ, 317, 593
De Young, D. S., Lind, K., & Strom, S. E. 1983, PASP, 95, 401
Duvert, G., Cernicharo, J., & Baudry, A. 1986, A&A, 164, 349
Ebert, R. 1955, Z. Astrophys., 37, 222
Elmegreen, B. G. 1987, in Interstellar Processes, ed. D. J. Hollenbach & H. A. Thronson (Dordrecht: Reidel), 259
Elmegreen, B. G. 1989, ApJ, 338, 178
Faber, S. M., & Gallagher, J. S. 1979, ARA&A, 17, 135
Fabricant, D., Lecar, M., & Gorenstein, P. 1980, ApJ, 241, 552
Fall, S. M., & Rees, M. J. 1977, MNRAS, 181, 37P
———. 1985, ApJ, 298, 18
———. 1988, in IAU Symp. 126, Globular Cluster Systems in Galaxies, ed. J. E. Grindlay & A. G. D. Philip (Dordrecht: Reidel), 323
Ferguson, H. C. 1989, AJ, 98, 367
Ferguson, H. C., & Sandage, A. 1991, AJ, 101, 765
Field, G. B., & Saslaw, W. C. 1965, ApJ, 142, 568
Fischer, P., Welch, D. L., Côté, P., Mateo, M., & Madore, B. F. 1992, AJ, 103, 857
Fleck, R. C., Jr. 1988, ApJ, 328, 299
Freeman, K. C. 1993, in ASP Conf. Ser. 48, The Globular Cluster–Galaxy Connection, ed. G. Smith & J. Brodie (San Francisco: ASP), 608
Friberg, P., & Hjalmarson, A. 1990, in Molecular Astrophysics, ed. T. W. Hartquist (Cambridge Univ. Press), 3
Goldsmith, P. F. 1987, in Interstellar Processes, ed. D. J. Hollenbach & H. A. Thronson (Dordrecht: Reidel), 51
Gratton, R. G., & Ortolani, S. 1989, A&AS, 73, 137
Harris, W. E. 1976, AJ, 81, 1095
Harris, W. E. 1991, ARA&A, 29, 543
———. 1993, in ASP Conf. Ser. 48, The Globular Cluster–Galaxy Connection, ed. G. Smith & J. Brodie (San Francisco: ASP), 472
Harris, W. E., Allwright, J. W. B., Pritchet, C. J., & van den Bergh, S. 1991, ApJS, 76, 115
Harris, W. E., Pritchet, C. J., & McClure, R. D. 1993, in ASP Conf. Ser. 48, The Globular Cluster–Galaxy Connection, ed. G. Smith & J. Brodie (San Francisco: ASP), 572
Harris, W. E., & van den Bergh, S. 1981, AJ, 86, 1627
Helfer, T. T., & Blitz, L. 1993, ApJ, 429, 86
Holtzman, J. A., et al. 1992, AJ, 103, 691
Johansson, L. E. B. 1991, in IAU Symp. 146, Dynamics of Galaxies and Their Molecular Cloud Distributions, ed. F. Combes & F. Casoli (Dordrecht: Kluwer), 1
Johnstone, D. 1993, AJ, 105, 155
Kang, H., Shapiro, P. R., Fall, S. M., & Rees, M. J. 1990, ApJ, 363, 488
Katz, N. 1992, ApJ, 391, 502
Kennicutt, R. C. 1989, ApJ, 344, 685
Kwan, J. 1979, ApJ, 229, 567
Kwan, J., & Valdes, F. 1983, ApJ, 271, 604
Lada, C. J., Margulis, M., & Dearborn, D. 1984, ApJ, 285, 141
Lada, E., Bally, J., & Stark, A. A. 1991, ApJ, 368, 432
Larson, R. B. 1981, MNRAS, 194, 809
———. 1990, PASP, 102, 709
———. 1992, in Star Formation in Stellar Systems, ed. G. Tenorio-Tagle, M. Prieto, & F. Sanchez (Cambridge Univ. Press), 125
Larson, R. B. 1993, in ASP Conf. Ser. 48, The Globular Cluster–Galaxy Connection, ed. G. Smith & J. Brodie (San Francisco: ASP), 675
Lee, H. M., Fahlman, G. G., & Richer, H. B. 1991, ApJ, 366, 455
Lee, Y.-W. 1992a, PASP, 104, 798
———. 1992b, AJ, 104, 1780
Leonard, P. J. T., Richer, H. B., & Fahlman, G. G. 1992, AJ, 104, 2104
Lilly, S. J. 1988, ApJ, 333, 161
Lutz, D. 1991, A&A, 245, 31
Mandushev, G., Spassova, N., & Staneva, A. 1991, A&A, 252, 94
Mateo, M. 1993, in ASP Conf. Ser. 48, The Globular Cluster–Galaxy Connection, ed. G. Smith & J. Brodie (San Francisco: ASP), 387
McKee, C. F. 1989, ApJ, 345, 782
McKee, C. F., Zweibel, E. G., Goodman, A. A., & Heiles, C. 1993, in Protostars and Planet III, ed. M. Matthews & E. Levy (Tucscon: Univ. of Arizona Press), 327
McLaughlin, D. E. 1994, PASP, 106, 47
McLaughlin, D. E., Harris, W. E., & Hanes, D. A. 1994, ApJ, 422, 486
Meurer, G. R., Freeman, K. C., Dopita, M. A., & Cacciari, C. 1992, AJ, 103, 60
Murray, S. D., & Lin, D. N. C. 1992, ApJ, 400, 265
———. 1993, in ASP Conf. Ser. 48, The Globular Cluster–Galaxy Connection, ed. G. Smith & J. Brodie (San Francisco: ASP), 738
Myers, P., & Goodman, A. A. 1988, ApJ, 329, 392
Oh, K.-S., & Lin, D. N. C. 1992, ApJ, 386, 519

Ostriker, J. P. 1988, in IAU Symp. 126, Globular Cluster Systems in Galaxies, ed. J. E. Grindlay, & A. G. D. Philip (Dordrecht: Kluwer), 271
Ostrov, P., Geisler, D., & Forte, J. C. 1993, AJ, 105, 1762
Peebles, P. J. E., & Dicke, R. H. 1968, ApJ, 154, 891
Pudritz, R. E. 1990, in IAU Symp. 140, Galactic and Intergalactic Magnetic Fields, ed. R. Beck, P. P. Kronberg, & R. Wielebinski (Dordrecht: Kluwer), 519
Pudritz, R. E., & Silk, J. 1989, ApJ, 342, 650
Racine, R. 1980, in IAU Symp. 85, Star Clusters, ed. J. E. Hesser (Dordrecht: Reidel), 369
Racine, R. 1991, AJ, 101, 865
Racine, R., & Harris, W. E. 1992, AJ, 104, 1068
Rand, R. J. 1992, AJ, 103, 815
Reed, L. G., Harris, G. L. H., & Harris, W. E. 1992, AJ, 103, 824
Richer, H. B., Crabtree, D. R., Fabian, A. C., & Lin, D. N. C. 1993, AJ, 105, 877
Richer, H. B., Fahlman, G. G., Buonanno, R., Fusi Pecci, F., Searle, L., & Thompson, I. B. 1991, ApJ, 381, 147
Richtler, T. 1992, Habilitationsschrift zur Erlangung, Sternwarte der Universitat Bonn
Rubio, M., Lequeux, J., & Boulanger, F. 1993, A&A, 271, 9
Saha, A. 1985, ApJ, 289, 310
Sandage, A., & Binggeli, B. 1984, AJ, 89, 919
Sanders, D. B., Scoville, N. Z., & Solomon, P. M. 1985, ApJ, 289, 373 (SSS)
Sarajedini, A., & King, C. R. 1989, AJ, 98, 1624
Scoville, N. Z., & Sanders, D. B. 1987, in Interstellar Processes, ed. D. J. Hollenbach & H. A. Thronson (Dordrecht: Reidel), 21
Scowen, P. A., Dufour, R. J., & Hester, J. J. 1992, AJ, 104, 92
Searle, L., & Zinn, R. 1978, ApJ, 225, 357
Secker, J. 1992, AJ, 104, 1472
Secker, J., & Harris, W. E. 1993, AJ, 105, 1358
Shapiro, P. R., & Kang, H. 1987, ApJ, 318, 32
Spergel, D. N., & Blitz, L. 1992, Nature, 357, 665
Stetson, P. B., VandenBerg, D. A., Bolte, M., Hesser, J. E., & Smith, G. H. 1989, AJ, 97, 1360
Suntzeff, N. 1993, in ASP Conf. Ser. 48, The Globular Cluster–Galaxy Connection, ed. G. Smith & J. Brodie (San Francisco: ASP), 167
Surdin, V. G. 1979, Soviet Astron., 23, 648
Tatematsu, K., et al. 1993, ApJ, 404, 643
Tonry, J. L., Ajhar, E. A., & Luppino, G. A. 1990, AJ, 100, 1416
VandenBerg, D. A., Bolte, M. J., & Stetson, P. B. 1990, AJ, 100, 445
van den Bergh, S. 1993, AJ, 105, 971
van den Bergh, S., Morbey, C., & Pazder, J. 1991, ApJ, 375, 594
Webbink, R. F. 1985, in IAU Symp. 113, Dynamics of Star Clusters, ed. J. Goodman & P. Hut (Dordrecht: Reidel), 541
Welter, G. L., Perry, J. J., & Kronberg, P. P. 1984, ApJ, 279, 19
West, M. J. 1993, MNRAS, 265, 755
Wilson, C. D., & Scoville, N. 1990, ApJ, 363, 435
Zinn, R. 1980, ApJ, 241, 602
———. 1985, ApJ, 293, 424
———. 1993a, in ASP Conf. Ser. 48, The Globular Cluster–Galaxy Connection, ed. G. Smith & J. Brodie (San Francisco: ASP), 38
———. 1993b, in ASP Conf. Ser. 48, The Globular Cluster–Galaxy Connection, ed. G. Smith & J. Brodie (San Francisco: ASP), 302